Paired-spike interactions and synaptic efficacy of retinal inputs to the thalamus

W. Martin Usrey, John B. Reppas & R. Clay Reid

Department of Neurobiology, Harvard Medical School, 220 Longwood Avenue, Boston, Massachusetts, 02115, USA

In many neural systems studied *in vitro*, the timing of afferent impulses affects the strength of postsynaptic potentials[1,2]. The influence of afferent timing on postsynaptic firing *in vivo* has received less attention. Here we study the importance of afferent spike timing *in vivo* by recording simultaneously from ganglion cells in the retina and their targets in the lateral geniculate nucleus of the thalamus. When two spikes from a single ganglion-cell axon arrive within 30 milliseconds of each other, the second spike is much more likely than the first to produce a geniculate spike, an effect we call paired-spike enhancement. Furthermore, simultaneous recordings from a ganglion cell and two thalamic targets indicate that paired-spike enhancement increases the frequency of synchronous thalamic activity. We propose that information encoded in the high firing rate of an individual retinal ganglion cell becomes distributed among several geniculate neurons that fire synchronously. Because synchronous geniculate action potentials are highly effective in driving cortical neurons[3], it is likely that information encoded by this strategy is transmitted to the next level of processing.

We made simultaneous recordings from 205 pairs of neurons in the cat; one neuron of each pair was in the retina and the other was in the lateral geniculate nucleus (LGN). Because retinal ganglion cells have high firing rates and are highly effective in driving geniculate neurons[4–7], this pathway is well suited for the detailed analysis of extracellular data. We mapped receptive fields using a random, computer-generated stimulus[8–10]. An example of the receptive fields of two simultaneously recorded neurons (off-centre X cells), one in the retina and the other in the LGN, is shown in Fig. 1a, b.

The raster plot in Fig. 1c shows the occurrence of geniculate spikes relative to 300 successive ganglion-cell spikes, each centred at time zero. Following a retinal spike, there was a clear tendency for the geniculate cell to generate a spike with a peak delay of 4.8 ms—a delay consistent with a monosynaptic connection[4,5]. This short latency peak is best appreciated in the cross-correlogram (Fig. 1d)—the average of the raster plots shown in Fig. 1c over all retinal spikes[4,5]. Of the 205 pairs of cells in this study, 12 had statistically significant[11] narrow correlogram peaks, indicative of monosynaptic connections.

We next determined whether the efficacy of a retinal spike (the probability of evoking a geniculate spike) was influenced by preceding patterns of retinal activity. Patterns of firing were characterized by two temporal parameters—interspike interval and dead time—that defined a pair of retinal spikes. In each pair, the second spike followed the first by a specific interspike interval (ISI) and the first spike was preceded by a minimum period of silence (dead time). The dead time ensured a comparable level of activity immediately preceding all first spikes. For example (Fig. 1e, f), we selected all pairs of retinal spikes that occurred 10.0 ± 0.4 ms apart and followed a dead time of at least 20.0 ms. As seen either as a raster plot (Fig. 1e) or as a paired-spike cross-correlogram (Fig. 1f), second retinal spikes were significantly more effective. We call this effect paired-spike enhancement, to distinguish it from other previously described effects such as paired-pulse facilitation.

The degree of paired-spike enhancement depended on both

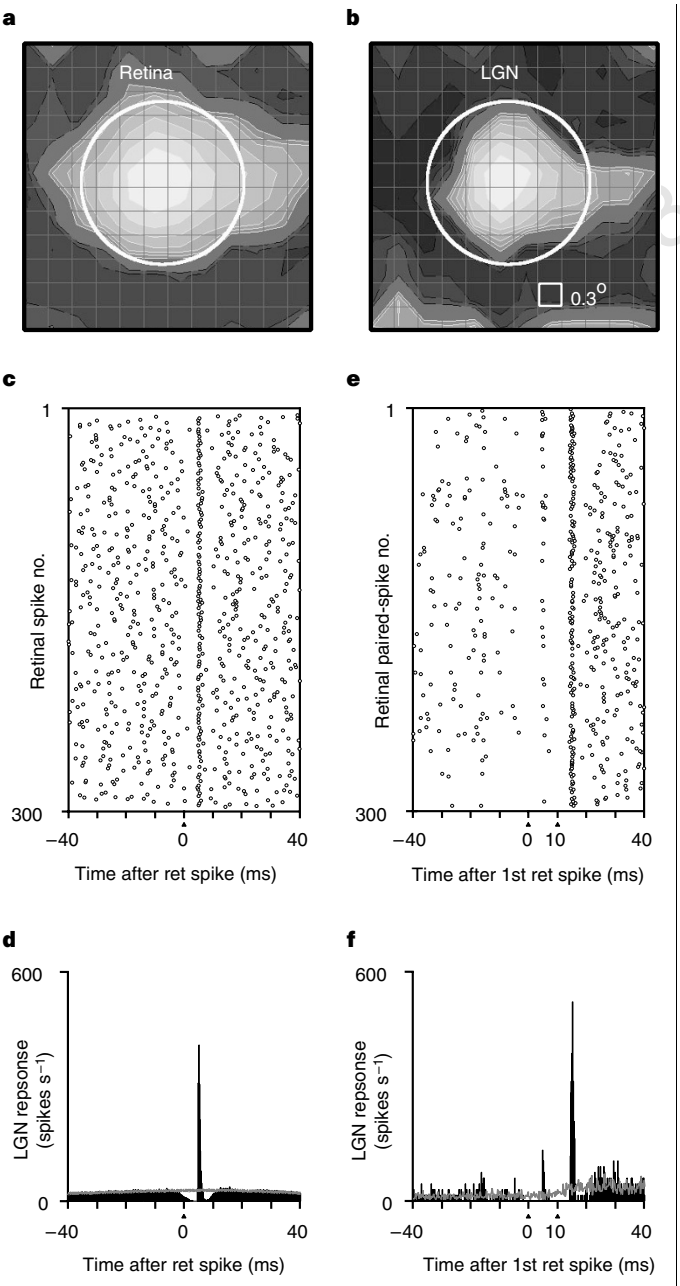

Figure 1 Recording of connected neurons in retina and LGN. **a**, **b**, Receptive fields of a retinal ganglion cell and geniculate neuron (on-centre X cells) mapped with white noise[8–10]. Bright regions were excited by bright stimuli, and dark regions by dark stimuli (pixel size 0.3°). Stimulus-response delay shown: 15–31 ms for retina, 31–46 ms for LGN. Circles represent a gaussian fit to the retinal receptive field (radius: $2.5\sigma_{ret}$). **c**, Raster plot of geniculate firing (stimulated by drifting grating) relative to 300 retinal spikes. The geniculate neuron often fired ~5 ms after the retinal spike. **d**, Cross-correlogram, which is equivalent to the sum of all rows of the raster plot (**c**); units are LGN spikes per second following an average retinal spike. The narrow, short-latency peak (above the stimulus-dependent shuffle correlogram[30] (grey line) indicates that the retinal ganglion cells provided monosynaptic input to the geniculate neuron[4,5]. Total time 797 s. Retinal spikes: 31,315; LGN spikes: 10,749. Retinal efficacy: 29.7% (see Methods). **e**, Raster plot of geniculate firing relative to 300 pairs of retinal spikes, each separated by 10.0 ± 0.2 ms and preceded by at least 20.0 ms of dead time. More geniculate spikes followed second retinal spikes than followed first retinal spikes. **f**, Cross-correlogram between paired retinal spikes and LGN. Number of retinal paired spikes is 336. Efficacy of first spikes (peak 1), 8.6%. Efficacy of second spikes (peak 2), 47.0%.

temporal parameters: interspike interval and dead time. The effect of varying the interspike interval was clear: the efficacy of second spikes reached a maximum at short intervals (~2–5 ms) and declined smoothly for intervals up to ~30 ms. This was found during excitation by a grating stimulus (Fig. 2a, d), by a white-noise stimulus (Fig. 2b, d), or in the absence of a visual stimulus (Fig. 2c).

We next studied the consequences of varying the dead time preceding the first spike. As would be expected, the average efficacy of first spikes (Fig. 2e) depended on the dead time preceding it; 5.4% efficacy was found when dead times were greater than 5 ms, and 1.8% efficacy was found for dead times of more than 30 ms. More important, varying the dead time also affected the peak efficacy of second spikes (Fig. 2f); efficacy decreased from 15.2% for dead times of more than 5 ms to 11.5% for dead times of more than 30 ms. Thus, the efficacy of a retinal spike is influenced not only by the immediately preceding spike, but also by the earlier level of activity. Regardless of the preceding dead time, however, the efficacy of second spikes was always much greater than the efficacy of first spikes.

All monosynaptic connections between the retina and the LGN, both strong and weak, showed paired-spike enhancement. The scatter plot in Fig. 3 shows the efficacy of second versus first retinal spikes for each cell pair ($n = 12$), averaged over all interspike intervals between 4 and 30 ms. All but one of the points fall above the line of unit slope, indicating that second spikes were more effective than first spikes in driving a geniculate response.

Our results show that when two retinal spikes occur within ~3–30 ms of each other, the second spike has an increased probability of evoking a postsynaptic spike. Whether this effect is the result of presynaptic mechanisms, such as calcium accumulation[2,12,13], or postsynaptic mechanisms, such as passive integration[14], cannot be determined from extracellular data. As most central synapses studied *in vitro* exhibit paired-pulse facilitation or depression (which rely on presynaptic mechanisms)[1,2], we predict that the effect is at least partially presynaptic. Paired-spike enhancement is unlikely to be a polysynaptic phenomenon, either cortical or intrathalamic, because of its fast onset; the effect is usually maximal at the shortest intervals that we can study, about 3 ms (determined by retinal relative refractory period). Furthermore, the effect is present without visual stimulation (Fig. 2c), when cortical feedback neurons are relatively silent. Finally, because some LGN neurons receive input from up to four ganglion cells[4,5,15], paired-spike enhancement might rely on other retinal inputs. This is unlikely, however, because it is seen when a single retinal ganglion cell drives almost all thalamic spikes (up to 82%; Fig. 2a–c).

Although it is likely that there is a presynaptic component to

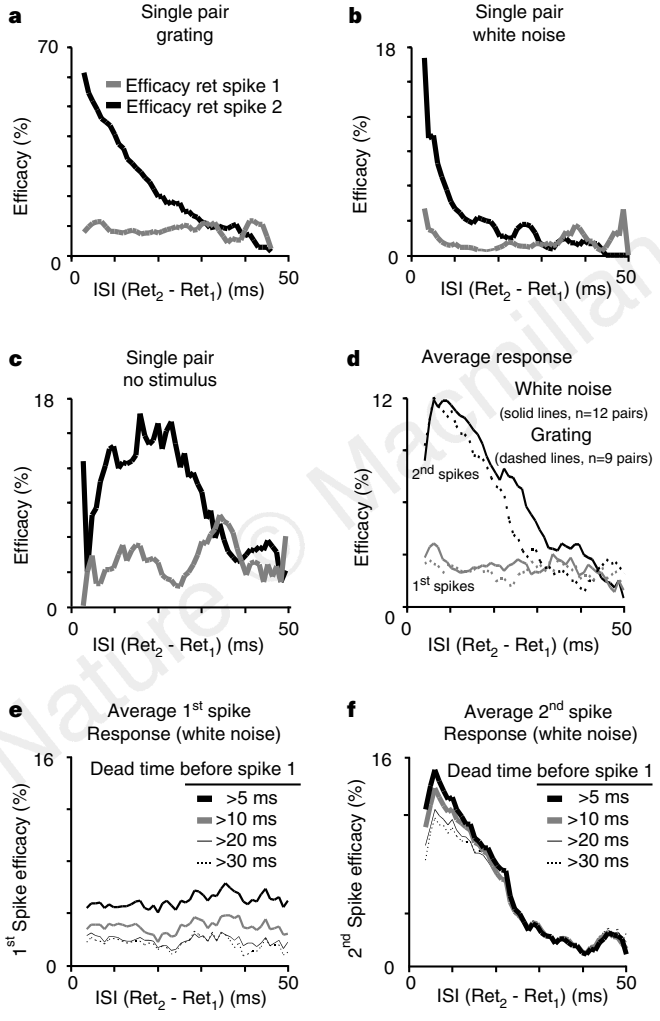

Figure 2 Time course and magnitude of paired-spike enhancement. **a**–**d**, Efficacy of pairs of retinal spikes (per cent that evoked a geniculate spike) that occurred at different interspike intervals (ISIs) following dead times of >20 ms. Grey lines indicate the efficacy of first retinal spikes; black lines indicate the efficacy of second retinal spikes. Efficacy at each retinal ISI was calculated as for Fig. 1, then smoothed with a 4-ms boxcar average. **a**–**c**, Efficacy profiles for a single retinogeniculate pair (the same pair as in Fig. 1) when **a**, excited by a grating, **b**, excited by white noise, or **c**, without visual stimulation (eyes covered). **d**, Average efficacy profiles for all pairs, excited with grating (9 pairs, dashed lines) or white noise (12 pairs, solid lines). **e**, **f**, Dependence of efficacies of first (**e**) and second (**f**) spikes on the dead time preceding the first spike. Curves were indistinguishable for dead times of >20 ms and >30 ms (as well as for >50 ms, not shown).

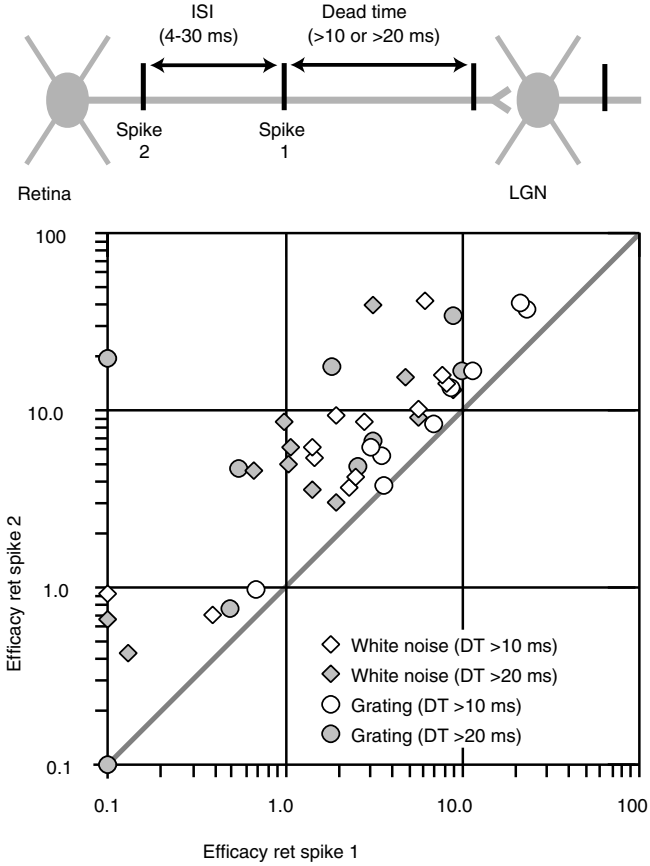

Figure 3 Scatter plot of efficacies of second versus first retinal spikes; all retinogeniculate connections showed paired-spike enhancement. Efficacies were averaged over an ISI range of 4–30 ms, weighted by number of occurrences of each ISI. Diamonds, white-noise stimuli; circles, grating stimuli. Dead time (DT) was either >10 ms (unfilled symbols) or >20 ms (filled symbols). Points on either axis are for efficacies <0.1%.

paired-spike enhancement, it almost certainly involves a dynamic interplay between facilitation and depression. Most classic studies of facilitation and depression *in vitro*[1,2] have relied on protocols in which pairs of stimuli are delivered on a quiescent baseline, or in which trains of spikes are elicited at constant rates. Several later studies[16–19] have used more naturalistic presynaptic spike trains, similar to those found *in vivo*, and found that synaptic efficacy depends, in a complex way, on the local temporal structure of the input. Although naturalistic spike trains, delivered *in vitro*, are important in understanding the mechanisms of synaptic modulation, the functional significance of these mechanisms can only be fully appreciated *in vivo*, when they occur in the context of the normal activity of the intact nervous system.

We next determined how paired-spike enhancement affects the activity of ensembles of thalamic neurons, particularly synchronous firing. Because retinal ganglion cells diverge anatomically to contact several thalamic targets[15,20], tightly synchronous activity of geniculate neurons by common input was predicted[21] well before it was observed[3]. Synchronous geniculate spikes are of particular interest, as they are more effective at driving cortical responses[3]. Here we have found that synchronous firing in the LGN is caused by retinal divergence, but also that paired-spike enhancement increases the number of synchronous events.

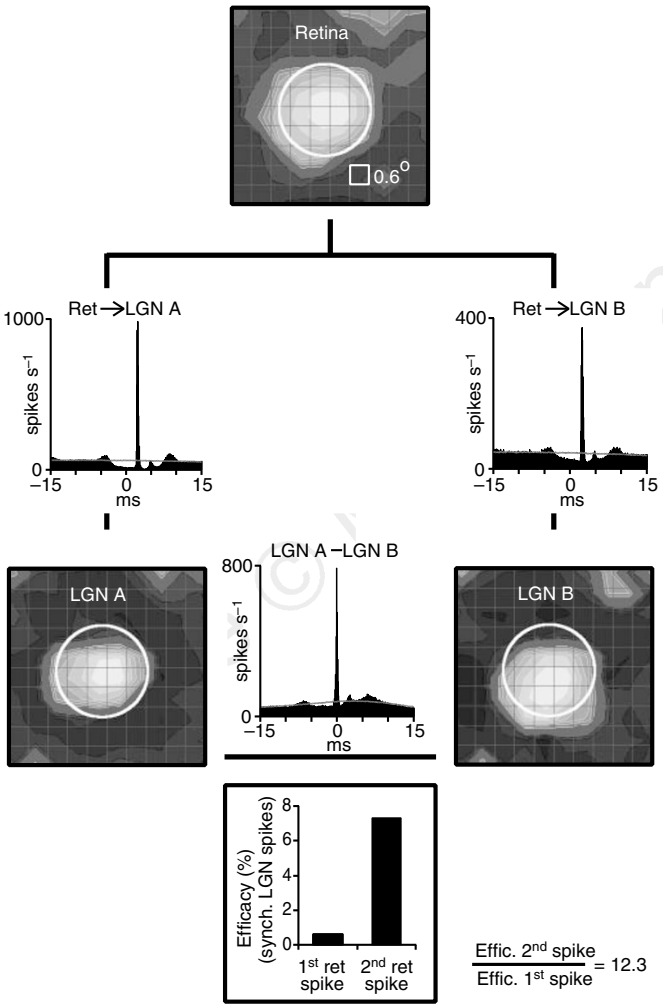

Figure 4 Divergent input from a single retinal ganglion cell synchronizes two geniculate neurons; paired-spike enhancement increases the frequency of this synchronization. The receptive fields of three simultaneously recorded on-centre Y cells (Retina, LGN A and LGN B) are shown. Circles represent the Gaussian fit to the retinal receptive field (radius: $2.5\sigma_{ret}$). Correlograms at the sides of the figure (Ret → LGN A; Ret → LGN B) have strong and narrow monosynaptic peaks, displaced ~2.5 ms to the right of zero. The lower correlogram (LGN A – LGN B) indicates that the geniculate cells fired many of their spikes synchronously (within 1.0 ms, centred at time zero). 84% of the synchronous spikes in the two geniculate cells occurred 2.5 ± 1.0 ms after a spike in the retinal cell. The histogram at the bottom shows the efficacy of first and second retinal spikes (ISI, 3–30 ms; dead time > 20 ms) in evoking synchronous geniculate spikes. Second retinal spikes were 12.3 times more likely than first spikes to evoke synchronous geniculate spikes.

Because we used a multielectrode array to record from the LGN, we were able twice to record simultaneously from two synchronized geniculate neurons and from a common retinal input. In one such example (Fig. 4), the receptive fields of one retinal cell and two simultaneously recorded geniculate cells all overlapped. The strong and narrow peaks (<1 ms) in the retinogeniculate correlograms (Ret → LGN A; Ret → LGN B) indicate that the two geniculate cells both received input from the retinal cell. As a result of this common input, the two geniculate cells fired many of their spikes synchronously (Fig. 4, LGN A–LGN B). In this case, the retinal cell drove 84% of the simultaneous spikes between LGN cells A and B.

How does paired-spike enhancement influence the relative incidence of synchronous LGN spikes? In this case, second retinal spikes were 12.3 times more likely than first spikes to evoke synchronous geniculate responses (Fig. 4, bottom). For the other three-cell recording, second retinal spikes were 1.75 times more effective in evoking synchronous geniculate spikes. Thus, as would be expected from the paired-spike effect on the activity of a single geniculate neuron, paired-spike enhancement increases the occurrence of synchronous spikes in geniculate neurons.

Correlated spiking of LGN cells is important for cortical development[22–24], but may also play a role in information coding (compare refs 25 and 26). In particular, synchronous geniculate spikes convey information beyond that conveyed by non-synchronous spikes[25]. Similarly, extra information is conveyed by the retina during periods of very high spike rate[27]. With paired-spike enhancement, this information may be selectively transmitted to the LGN, in particular to synchronous spikes. Thus there is a partial transition from a rate code to a synchronous population code.

Paired-spike enhancement, together with divergent connections from one retinal cell onto several geniculate neurons, works to increase the number of synchronous spikes in the LGN. Further, synchronous geniculate spikes can interact synergistically in evoking cortical spikes (compare ref. 3 with refs 28, 29). Thus, two aspects of the anatomy of the visual pathway—divergent input to the LGN and reconvergent input to the visual cortex—have physiological counterparts, namely thalamic synchrony and thalamocortical synergy, respectively. This interplay of anatomy and physiology acts not only to reinforce the pathway from periphery to cortex, but also to provide the cortex with more information about the visual environment. □

Methods

Cats were prepared for electrophysiological recordings as described[3,11]. Recordings in the Alaminae of the dorsal LGN were made with a seven-electrode array (Thomas Recording, Marburg). Retinal recordings were made with single electrodes (AM Systems) inserted into the eye through a guide tube. Spike isolation was confirmed with off-line waveform analysis (DataWave Systems); the presence of a refractory period in autocorrelations; and observations of analogue data recorded on tape. The significance of correlogram peaks was assessed using the method of ref. 11, but with a bandpass filter of 350–2,100 Hz to capture the very fast peaks. The peak integral was determined from unfiltered correlograms (2.0-ms range around maximum), minus the baseline (taken from 2-ms ranges immediately before and after the peak range). The efficacy of retinal spikes was defined as: (peak integral)/(total retinal spikes).

Received 12 June; accepted 3 August 1998.

1. Magleby, K. L. in *Synaptic Function* (eds Edelman, G. M., Gall, W. E. & Cowan, W. M.) 21–56 (Wiley, New York, 1987).
2. Zucker, R. S. Short-term synaptic plasticity. *Annu. Rev. Neurosci.* **12,** 13–31 (1989).

3. Alonso, J.-M., Usrey, W. M. & Reid, R. C. Precisely correlated firing in cells of the lateral geniculate nucleus. *Nature* **383,** 815–819 (1996).
4. Cleland, B. G., Dubin, M. W. & Levick, W. R. Sustained and transient neurones in the cat's retina and lateral geniculate nucleus. *J. Physiol.* **217,** 473–496 (1971).
5. Cleland, B. G., Dubin, M. W. & Levick, W. R. Simultaneous recording of input and output of lateral geniculate neurones. *Nature New Biol.* **231,** 191–192 (1971).
6. Hubel, D. H. & Wiesel, T. N. Integrative action in the cat's lateral geniculate body. *J. Physiol.* **155,** 385–398 (1961).
7. Kaplan, E., Purpura, K. & Shapley, R. M. Contrast affects the transmission of visual information thrugh the mammalian lateral geniculate nucleus. *J. Physiol.* **391,** 267–288 (1987).
8. Reid, R. C., Victor, J. D. & Shapley, R. M. The use of m-sequences in the analysis of visual neurons: linear receptive field properties. *Vis. Neurosci.* **14,** 1015–1027 (1997).
9. Sutter, E. E. in *Advanced Methods of Physiological Systems Modeling* Vol. 1 (ed. Marmarelis, V.) 303–315 (Univ. Southern California, Los Angeles, 1987).
10. Sutter, E. E. in *Nonlinear Vision: Determination of Neural Receptive Fields, Function and Networks* (eds Pinter, R. & Nabet, B.) 171–220 (CRC, Cleveland, 1992).
11. Reid, R. C. & Alonso, J.-M. Specificity of monosynaptic connections from thalamus to visual cortex. *Nature* **378,** 281–284 (1995).
12. Katz, B. & Miledi, R. The role of calcium in neuromuscular facilitation. *J. Physiol.* **195,** 481–492 (1968).
13. Atluri, P. P. & Regehr, W. G. Determinants of the time course of facilitation at the granule cell to Purkinje cell synapse. *J. Neurosci.* **16,** 5661–5671 (1996).
14. Bloomfield, S. A., Hmaos, J. E. & Sherman, S. M. Passive cable properties and morphological correlates of neurones in the lateral geniculate nucleus of the cat. *J. Physiol.* **383,** 653–692 (1987).
15. Hamos, J. E., Van Horn, S. C., Raczkowski, D. & Sherman, S. M. Synaptic circuits involving an individual retinogeniculate axon in the cat. *J. Comp. Neurol.* **259,** 165–192 (1987).
16. Varela, J. A. *et al*. A quantitative description of short-term plasticity at excitatory synapses in layer 2/3 of rat primary visual cortex. *J. Neurosci.* **17,** 7926–7940 (1997).
17. Tsodyks, M. V. & Markram, H. The neural code between neocortical pyramidal neurons depends on neurotransmitter release probability. *Proc. Natl Acad. Sci. USA* **94,** 719–723 (1997).
18. Markram, H. & Tsodyks, M. Redistribution of synaptic efficacy between neocortical pyramidal neurons. *Nature* **382,** 807–810 (1996).
19. Abbott, L. F., Varela, J. A., Sen, K. & Nelson, S. B. Synaptic depression and cortical gain control. *Science* **275,** 220–224 (1997).
20. Peters, A. & Payne, B. R. Numerical relationships between geniculocortical afferents and pyramidal cell modules in cat primary visual cortex. *Cereb. Cortex* **3,** 69–78 (1993).
21. Cleland, B. G. in *Visual Neuroscience* (eds Pettigrew, J. D., Snaderson, K. S. & Levick, W. R.) 111–120 (Cambridge Univ. Press, London, 1986).
22. Meister, M., Wong, R. O., Baylor, D. A. & Shatz, C. J. Synchronous bursts of action potentials in ganglion cells of the developing mammalian retina. *Science* **252,** 939–943 (1991).
23. Miller, K. D. A model for the development of simple cell receptive fields and the ordered arrangement of orientation columns through activity-dependent competition between ON- and OFF-center inputs. *J. Neurosci.* **14,** 409–441 (1994).
24. Weliky, M. & Katz, L. C. Disruption of orientation tuning in visual cortex by artificially correlated neuronal activity. *Nature* **386,** 680–658 (1997).
25. Dan, Y., Alonso, J.-M., Usrey, W. M. & Reid, R. C. Coding of visual information by precisely correlated spikes in the lateral geniculate nucleus. *Nature Neurosci.* (in the press).
26. Meister, M., Lagnado, L. & Baylor, D. A. Concerted signaling by retinal ganglion cells. *Science* **270,** 1207–1210 (1995).
27. Smirnakis, S. M., Warland, D. K., Berry, M. J. & Meister, M. Spike bursts in visual responses of retinal ganglion cells. *Soc. Neurosci. Abstr.* **22,** 494 (1996).
28. König, P., Engel, A. K. & Singer, W. Integrator or coincidence detector? The role of the cortical neuron revisited. *Trends Neurosci.* **19,** 130–137 (1996).
29. Usrey, W. M. & Reid, R. C. Synchronous activity in the visual system. *Annu. Rev. Physiol.* (in the press).
30. Perkel, D. H., Gerstein, G. L. & Moore, G. P. Neuronal spike trains and stochastic point processes. II. Simultaneous spike trains. *Biophys. J.* **7,** 419–440 (1967).

Acknowledgements. This work was supported by the NIH, The Klingenstein Fund, The Harvard Mahoney Neuroscience Institute, and The Howard Hughes Medical Institute. We thank E. Serra for technical assistance and J.-M. Alonso, J. Assad, M. Livingstone, M. Meister, W. Regehr and D. Hubel for comments on this manuscript.

Correspondence and requests for materials should be addressed to R.C.R. (e-mail: clay_reid@hms.harvard.edu).

Drosophila oocyte localization is mediated by differential cadherin-based adhesion

Dorothea Godt & Ulrich Tepass

Department of Zoology, Unviersity of Toronto, 25 Harbord Street, Toronto, Ontario M5S 3G5, Canada
These authors contributed equally to this work

In a *Drosophila* follicle the oocyte always occupies a posterior position among a group of sixteen germline cells. Although the importance of this cell arrangement for the subsequent formation of the anterior–posterior axis of the embryo is well documented[1–4], the molecular mechanism responsible for the posterior localization of the oocyte was unknown. Here we show that the homophilic adhesion molecule *D*E-cadherin[5–7] mediates oocyte positioning. During follicle biogenesis, *D*E-cadherin is expressed in germline (including oocyte) and surrounding follicle cells, with the highest concentration of *D*E-cadherin being found at the interface between oocyte and posterior follicle cells. Mosaic analysis shows that *D*E-cadherin is required in both germline and follicle cells for correct oocyte localization, indicating that germline–soma interactions may be involved in this process. By analysing the behaviour of the oocyte in follicles with a chimaeric follicular epithelium, we find that the position of the oocyte is determined by the position of *D*E-cadherin-expressing follicle cells, to which the oocyte attaches itself selectively. Among the *D*E-cadherin positive follicle cells, the oocyte preferentially contacts those cells that express higher levels of *D*E-cadherin. On the basis of these data, we propose that in wild-type follicles the oocyte competes successfully with its sister germline cells for contact to the posterior follicle cells, a sorting process driven by different concentrations of *D*E-cadherin. This is, to our knowledge, the first *in vivo* example of a cell-sorting process that depends on differential adhesion mediated by a cadherin.

*D*E-cadherin, encoded by the gene *shotgun* (*shg*), is the major epithelial cadherin in *Drosophila* and forms a cell adhesion complex with Armadillo/β-catenin and *D*α-catenin[5–9]. During oogenesis, *D*E-cadherin is expressed in all germline and follicle cells in the germarium and the follicles (Fig. 1c). Before follicle formation, the oocyte accumulates more *D*E-cadherin than the other 15 germline cells (the nurse cells), which are connected to the oocyte by cytoplasmic bridges known as the ring canals. The higher level of *D*E-cadherin in the oocyte depends on oocyte specification as, in *egalitarian* (*egl*) mutants, in which all 16 germline cells develop into nurse cells[10,11], there are no differences in *D*E-cadherin concentrations between germline cells (Fig. 1f).

Follicle formation is initiated when follicle cells grow inwards at the posterior side of the germ cell cluster, which forms a monolayer resting on the follicle cells (Fig. 1a, b). Subsequently, the germ cell cluster rounds off and eventually becomes covered with follicle cells at its anterior side also. The oocyte, which initially has a variable position, always assumes the most posterior position during follicle formation. Higher levels of *D*E-cadherin are seen in the posterior and anterior follicle cells than in lateral follicle cells (Fig. 1d). However, the highest *D*E-cadherin concentration is seen at the interface between the oocyte and the posterior follicle cells (Fig. 1d, e). In *egl* mutants, anterior and posterior follicle cells also express increased *D*E-cadherin levels, but no anterior–posterior differences are seen (Fig. 1f). Increased *D*E-cadherin concentrations at the interface between the oocyte and posterior follicle cells are maintained until stage 7 of oogenesis. Armadillo is distributed similarly to *D*E-cadherin (Fig. 1g). The *D*E-cadherin expression pattern, together with the finding that *shg* mutant germ line clones fail to produce eggs[6], is consistent with a function for this adhesion molecule in both germline and follicle cells. In particular, the high accumulation of *D*E-cadherin at the interface of oocyte and posterior follicle cells indicates that it may mediate interactions between these two cell types.

To study the consequences of loss of *D*E-cadherin expression during oogenesis, we first analysed the semiviable allelic combination $shg^{P34\text{-}1}/shg^{R6}$. Mislocalization of the oocyte was seen in 29.5% of stage 7–9 mutant follicles ($n = 383$), compared with 0% in wild-type follicles ($n = 498$) (Fig. 2). To determine whether *D*E-cadherin is required in the germline or in the follicular epithelium for oocyte localization, and to analyse oogenesis in the absence of *D*E-cadherin expression, we generated cell clones homozygous for the null allele shg^{R69}. The most prominent phenotype of germline clones that lack *D*E-cadherin is a mislocalization of the oocyte (Fig. 3a, b, e, f). An abnormal position of the oocyte is seen already in stage 1 follicles and in 89% of follicles with a mutant germline (Fig. 3i). In addition to mislocalization of the oocyte, lack of *D*E-cadherin expression